

Diagonal superexchange in a simple square CuO₂ lattice

V. A. Gavrichkov,^{1,2} S. I. Polukeev,¹ and S. G. Ovchinnikov¹

¹*Kirensky Institute of Physics, Siberian Branch of the Russian Academy of Sciences, 660036 Krasnoyarsk, Russia*

²*Rome International Center for Materials Science Superstripes RICMASS, via del Sabelli 119A, 00185, Roma, Italy*

(Dated: February 6, 2025)

Many microscopic models with the interaction between the next-nearest neighbours as a key parameter for cuprate physics have inspired us to study the diagonal superexchange interaction in a CuO₂ layer. Our investigation shows that models with extended hopping provide a correct representation of magnetic interactions only in a hypothetical square CuO₂ layer, where the diagonal superexchange interaction with the next-nearest neighbors always has the AFM nature. The conclusions are based on the symmetry prohibition on FM contribution to the diagonal superexchange between the next-nearest neighbors for a simple square CuO₂ layer rather than for a real CuO₂ layer, where diagonal AFM superexchange may be overestimated. We also discuss the reasons for magnetic frustration effects and high sensitivity of spin nanoinhomogeneity to square symmetry breaking.

I. INTRODUCTION

The theory of superexchange interaction describes well both qualitatively and quantitatively the antiferromagnetic (AFM) interaction of nearest neighbor ions Cu²⁺ in the CuO₂ layer of parent cuprates (see works ¹⁻³ and references therein, including pressure and optical pumping effects ^{4,5}). However, The nature of hopping and superexchange with the next-nearest neighbors is less obvious and has been discussed for a long time ⁶⁻¹⁰.

These parameters are relevant in a number of approaches to studying the physics of high- T_c superconducting (HTSC) cuprates. Hopping and superexchange with the next-nearest neighbors could be important not only for the extended hopping problem in a set of t - J , t - t' - J , t - t' - t'' - J models with a realistic hole-pairing mechanism in HTSC cuprates (see ¹¹ and references therein), but also for understanding the nature of a pseudogap state with \vec{k} arcs in the antinodal direction of the Fermi surface in \vec{k} -dependent experiments^{12,13}. Moreover, it is known that the temperature window for the pseudogap state shrinks with the increasing next-nearest neighbor hopping, which indicates that diagonal hopping may not be supportive of the pseudogap features ¹⁴. The results of dynamic cluster quantum Monte Carlo simulations for the Lifshitz transition of the two-dimensional Hubbard model show the sensitivity to the magnitude of diagonal next-nearest neighbor hopping to be a control parameter ¹⁵. Complicated spectral features of the two-dimensional Hubbard model are simply interpreted near the Mott transition by considering how the next-nearest neighbor hopping shifts spectral weights¹⁶. The momentum-sector-selective metal-insulator transitions in the eight-site dynamical cluster approximation for the 2D Hubbard model are explored on a phase diagram in the space of interaction and second-neighbor hopping control parameters ¹⁷. The magnitude of the interaction of diagonal neighbors plays a key role in the study of spin (SDW) and charge(CDW) nanoinhomogeneity in cuprate materials, where both observed phases have tilted stripes

(the so called "Y shift") with the same degree of tilting ¹⁰, and the origin of tilting can be explained by a small anisotropy in hopping between the next-near neighbors. The specific alignment direction of the stripes is highly sensitive to the hopping interaction where even a small anisotropy in it can result in subtle observed tilting in LSCO ^{6,18,19} and LBCO ²⁰ samples.

However, the studies of the effects of next-nearest neighbor hopping and magnetic frustrations on the spectrum of quasiparticles are still based on assumptions regarding the sign and magnitude of hopping and superexchange interaction $J_{tot}(\vec{R}_{11})$ between the diagonal neighbors. It is certainly not enough to understand the whole range of phenomena associated with these parameters. In previous papers ^{4,21} we derived a simple rule for detecting the sign of contribution to the superexchange interaction from a single virtual electron-hole pair. However, our conclusions concerned only the interaction with the nearest neighboring magnetic ions. For the CuO₂ layer of parent cuprates, this magnitude $J_{tot}(\vec{R}_{01}) \approx 0.15eV$ ⁵ is in agreement with the neutron scattering data ³, and the approach itself allows us to study the dependence of superexchange in $3d$ oxides on external factors: applied pressure^{5,21} and optical pumping ²².

In parent cuprates, virtual hopping and electron-hole pairs on the (next-)nearest neighbors can also lead to superexchange between them. Here, we show the superexchange constant $J_{tot}(\vec{R}_{ij})$, important for other approaches, to behave in an unusual way. Indeed, it has a zero magnitude at the diagonal directions $\vec{R}_{ij} = \vec{R}_{11}$ of the square CuO₂ layer for the virtual electron-hole pair with the B_{1g} hole symmetry, where the corresponding $^3B_{1g}$ triplet band competes in energy with the Zhang-Rice singlet $^1A_{1g}$ band ^{5,23-25}. This leads exactly to a zero FM contribution to the total magnetic interaction $J_{tot}(\vec{R}_{11})$ between the next-nearest neighbors of Cu²⁺ ions. As a consequence, the latter has purely AFM na-

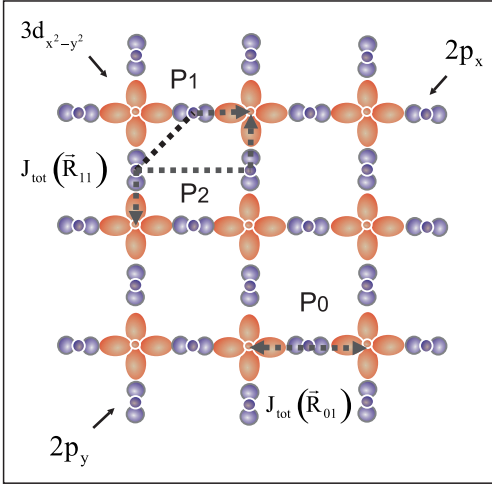


FIG. 1. Paths P_0 , P_1 and P_2 of the superexchange interactions $J_{tot}(\vec{R}_{01})$ and $J_{tot}(\vec{R}_{11})$ for the first and the second neighbor ions with the participation of $2p$ oxygen orbitals forming σ overlapping with $3d$ copper ions, and 90° (P_1) or small π (P_2) - overlapping between themselves. Here, the interactions $J_{tot}(\vec{R}_{01})$ are of AFM nature, but the magnitude of the $J_{tot}(\vec{R}_{11})$ interaction with the second neighbors is still unknown.

ture $J_{tot}(\vec{R}_{11}) < 0$, but it quickly decreases with the distance between the Cu^{2+} ions.

The paper is organized as follows: in the next section (Sec.II) we provide theoretical background on the many-electron approach to the study of superexchange interactions in parent cuprates. Symmetric effects on superexchange in the CuO_2 layer with the square symmetry are given in detail in Sec.III. Discussion and conclusion

are presented in Sec.IV.

II. HAMILTONIAN

In this section, we investigate the sign and magnitude of the superexchange interaction $J_{tot}(\vec{R}_{11})$ with next-nearest-neighbor Cu^{2+} ions through different oxygen orbitals in the CuO_2 layer (see Fig.1). Indeed, in the magnetic interaction with the second neighbors, the overlapping oxygen orbitals play a significant role. There are two paths P_1 and P_2 to create various virtual electron-hole pairs. They are distinguished by the overlapping oxygen orbitals. There are 90° degree overlapping oxygen orbitals in P_1 , and small π - overlapping in P_2 . The virtual electron-hole pairs in both paths can generate both AFM and FM contributions to the superexchange interaction $J_{tot}(\vec{R}_{11})$ between the diagonal second neighbor Cu^{2+} ions.

The superexchange constant $J_{tot}(\vec{R}_{ij})$ in Eq.(1) is additive over all possible states in the electronic N_+ ($|A_1\rangle$) and two-hole N_- ($|^1A_{1g}\rangle_{nS}, |^3B_{1g}\rangle_{mT}, \dots$) sectors in Fig.2, and the superexchange interaction (1) is obtained in the second order of the cell perturbation theory over interband contributions to the total Hamiltonian \hat{H} from the interatomic hopping contribution^{4,26,27}.

$$\hat{H}_S = \hat{H}_{AFM} + \hat{H}_{FM}, \quad (1)$$

where $\hat{H}_{AFM} = \sum_{ij} J_{AFM}(\vec{R}_{ij}) (\vec{s}_i \vec{s}_j - \frac{1}{4} n_i n_j)$, $\hat{H}_{FM} = \sum_{ij} J_{FM}(\vec{R}_{ij}) (\vec{s}_i \vec{s}_j + \frac{3}{4} n_i n_j)$, and the exchange constants $J_{AFM}(\vec{R}_{ij}) > 0$, $J_{FM}(\vec{R}_{ij}) < 0$ are given by

$$J_{AFM}(\vec{R}_{ij}) = \sum_{nS} J_{AFM}^{(nS)}(\vec{R}_{ij}) = \sum_{nS=1}^{N_S} |t^{0,nS}(R_{ij})|^2 / \Delta_{nS}, \quad \Delta_{nS} = E_{nS} + E_{1A} - 2\varepsilon_{b_{1g}} \quad (2)$$

$$J_{FM}(\vec{R}_{ij}) = \sum_{mT} J_{FM}^{(mT)}(\vec{R}_{ij}) = - \sum_{mT=1}^{N_T} |t^{0,mT}(R_{ij})|^2 / 2\Delta_{mT}, \quad \Delta_{mT} = E_{mT} + E_{1A} - 2\varepsilon_{b_{1g}}.$$

The total multi-electron Hamiltonian in the representa-

tion of the Hubbard operators²⁸, looks like $\hat{H} = \hat{H}_0 + \hat{H}_1$,^{29,30} where

$$\begin{aligned}
\hat{H}_0 &= \sum_i \left\{ (E_{1A^1A} - N_+\mu) X_i^{1A^1A} + (\varepsilon_{b_{1g}} - N_0\mu) X_i^{b_{1g}b_{1g}} + \sum_{h=nS, mT} (E_h - N_-\mu) X_i^{hh} \right\} \\
\hat{H}_1 &= \sum_{ij\sigma} \sum_{rr'} t_{\sigma}^{rr'} (\vec{R}_{ij}) X_i^{+r} X_j^{r'} \\
t_{\sigma}^{r,r'} (\vec{R}_{ij}) &= \sum_{ij} \sum_{\lambda\lambda'} \sum_{rr'} t_{\lambda\lambda'} (\vec{R}_{ij}) \gamma_{\lambda\sigma}^*(r) \gamma_{\lambda'\sigma}(r'),
\end{aligned} \tag{3}$$

and $\gamma_{\lambda\sigma}^*(r) = \langle h | c_{\lambda\sigma}^+ | b_{1g} \rangle$, where the index h runs over all possible two-hole states in the N_- sector for the material with magnetic ions Cu^{2+} in the d^9 electron configuration. Here, $X_i^{+r} = |h\rangle \langle b_{1g}| (|1A\rangle \langle b_{1g}|)$ is the Hubbard operators of creating holes(electrons) with the root vectors $r = (h, b_{1g})$. Virtual electron-hole excitations through the dielectric gap $\Delta_h = E_h + E_{1A} - 2\varepsilon_{b_{1g}}$ to the conduction band and vice versa in Eq.(2) contribute to the superexchange interaction \hat{H}_S ⁴:

$$\begin{aligned}
t^{0, nS} (R_{ij}) &\equiv t^{(1Ab_{1g}), (b_{1g}nS)} (R_{ij}) = \\
&= \sum_{\lambda\lambda'} t^{\lambda\lambda'} (R_{ij}) \gamma_{\lambda\sigma}^*(1Ab_{1g}) \gamma_{\lambda'\sigma}(b_{1g}nS) \\
t^{0, mT} (R_{ij}) &\equiv t^{(1Ab_{1g}), (b_{1g}mT)} (R_{ij}) = \\
&= \sum_{\lambda\lambda'} t^{\lambda\lambda'} (R_{ij}) \gamma_{\lambda\sigma}^*(1Ab_{1g}) \gamma_{\lambda'\sigma}(b_{1g}mT).
\end{aligned} \tag{4}$$

The spin Hamiltonian (1) was derived from the original Hamiltonian (3) by using the projective operator method^{4,27}. For details of deriving the multi-electron Hamiltonian from the multi-orbital pd model, see the works³¹⁻³³, where a five-orbital basis p_λ , ($\lambda = x, y, z$), $d_{x^2-y^2}$, d_{z^2} is typically used. All the possible eigenstates $|1A_{1g}\rangle_{nS}$ and $|3B_{1g}\rangle_{mT}$ in the configuration space in Fig.2, as well as their energies E_h with $h = nS, mT$ are obtained in the exact diagonalization procedure for the intra-cell part of the multi-orbital pd model³³. The sum of all the FM and AFM contributions corresponds to the sum over all possible virtual electron-hole pairs (the so called exchange loops²¹). The FM or AFM nature of the contribution from a specific exchange loop is easily determined using the rule: if $S_+ = S_-$ there is an AFM contribution, in the case of $S_+ = S_- \pm 1$ there is an FM contribution, where S_\pm is the spin of the electron and hole in the specific virtual pair^{21,34}[25,38]. All the triplet states $|mT\rangle$ in the hole sector $N_- (d^8)$ contribute $J_{FM}(\vec{R}_{ij})$, and all the singlet states $|nS\rangle$ contribute $J_{AFM}(\vec{R}_{ij})$ to the exchange constant $J_{tot}(\vec{R}_{ij})$. Thus, the dependence of the superexchange interaction on the distance between the interacting Cu ions in the CuO_2 layer can be calculated using $t^{0, nS}(\vec{R}_{ij})$ and $t^{0, mT}(\vec{R}_{ij})$ hopping integrals in Eq.(2).

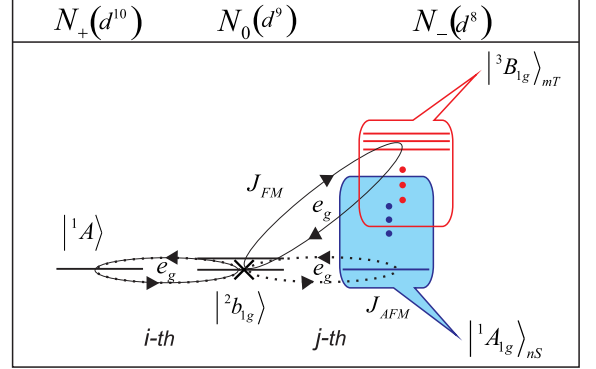


FIG. 2. Configuration space of the unit cell of the CuO_2 layer. The cross denotes the occupied hole eigenstates $|b_{1g}\rangle$ in the $N_0 (d^9)$ sector. The ellipses correspond to the virtual e_g electron-hole pairs with the $J_{FM}(\vec{R}_{ij})$ and $J_{AFM}(\vec{R}_{ij})$ contributions to the total exchange interaction \hat{H}_S .

III. DIAGONAL SUPEREXCHANGE INTERACTION IN THE SQUARE SYMMETRY OF THE CuO_2 LAYER

Where are the effects of the CuO_2 layer symmetry hidden in the calculation of the $J_{tot}(R_{11})$ exchange constant using Eq.(2)? To begin with, there is the point C_4 symmetry of the CuO_6 octahedron in the procedure of exact diagonalization of the intra-cell part of the Hamiltonian of the pd model³³. Indeed, there are $C_{2N_\lambda}^2 = N_S + 3N_T$ of the spin singlets $N_S = C_{N_\lambda}^2 + N_\lambda$ and triplets $N_T = C_{N_\lambda}^2$ in the two-hole $N_- (d^8)$ sector (Fig.2) within the N_λ orbital approach, where C_n^k is the number of combinations. For example, in the five-orbit approach there are 15 AFM ($N_S = 15$) and 10 FM ($N_T = 10$) contributions to the total superexchange interaction $J_{tot}(\vec{R}_{ij})$ from various virtual electron-hole pairs.

Using the intra-cell part of the multi-orbital pd Hamiltonian in the symmetric representation of canonical fermions³⁵ of all the spin singlet states $|1A_{1g}\rangle_{nS}$ and $|1B_{1g}\rangle_{mT}$, spin triplet states $|3A_{1g}\rangle_{nS}$ and $|3B_{1g}\rangle_{mT}$, and also single hole spin doublet states $|2a_{1g}\rangle$, $|2b_{1g}\rangle$ can be obtained in the exact diagonalization procedure for the eigenvalue problem in different sectors: $N_- (d^8)$, $N_0 (d^9)$, $N_+ (d^{10})$ of the configuration space. To solve

another problem associated with taking into account the common oxygen ion in the CuO_2 layer, the initial pd

Hamiltonian was rewritten in the representation of symmetrized Bloch $2p$ states of oxygen ions^{31–33,35}:

$$\begin{pmatrix} b_{\vec{k}\sigma} \\ a_{\vec{k}\sigma} \end{pmatrix} = \hat{P}(k_x, k_y) \begin{pmatrix} p_{x\vec{k}\sigma} \\ p_{y\vec{k}\sigma} \end{pmatrix} = i/\mu_{\vec{k}} \begin{pmatrix} s_x(\vec{k}) & s_y(\vec{k}) \\ \text{sgn}(k_x k_y) s_y(\vec{k}) & -\text{sgn}(k_x k_y) s_x(\vec{k}) \end{pmatrix} \begin{pmatrix} p_{x\vec{k}\sigma} \\ p_{y\vec{k}\sigma} \end{pmatrix}, \quad (5)$$

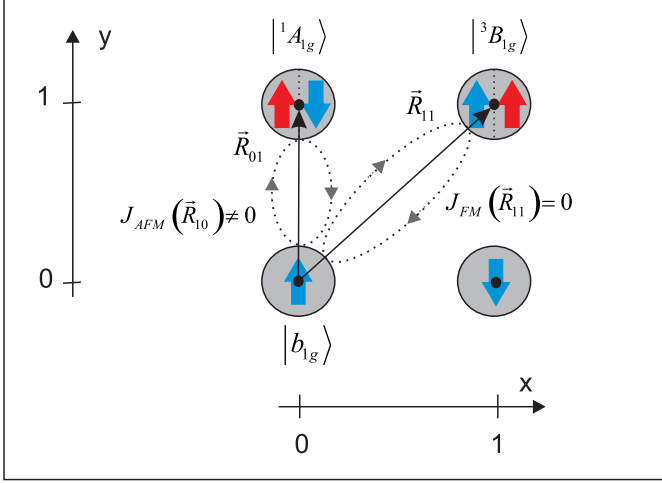


FIG. 3. A diagram of the direct and diagonal superexchange interactions in the cell representation in the simple square CuO_2 layer. Here, the ellipses show the virtual electron-hole pairs with the contributions $J_{FM}(\vec{R}_{ij})$ and $J_{AFM}(\vec{R}_{ij})$ to the total superexchange interaction $J_{tot}(\vec{R}_{ij})$.

where $|\hat{P}(k_x, k_y)|^2 = 1$, and the coefficients $\mu_{\vec{k}} = \sqrt{s_x^2(\vec{k}) + s_y^2(\vec{k})}$ with $s_x(\vec{k}) = \sin(k_x/2)$ and $s_y(\vec{k}) = \sin(k_y/2)$ constructed on the square lattice of the CuO_2 layer. As a consequence, the initial pd Hamiltonian in the cell representation of symmetrized Wannier states can be renormalized by using the coefficients $\lambda_{\vec{k}} = \frac{2s_x s_y}{\mu_{\vec{k}}}$, $\xi_{\vec{k}} = \frac{s_x^2 - s_y^2}{\mu_{\vec{k}}}$, for pd hopping and $\nu_{\vec{k}} = \frac{2s_x^2 s_y^2}{\mu_{\vec{k}}^2}$, $\chi_{\vec{k}} = \frac{2s_x s_y}{\mu_{\vec{k}}^2} (s_x^2 - s_y^2)$ for pp hopping, two of which $\xi(\vec{R}_{ij}) = \frac{1}{\sqrt{N}} \sum_{\vec{k}} \xi_{\vec{k}}$ and $\chi(\vec{R}_{ij})$ are equal to zero for diagonal hopping with $\vec{R}_{ij} = \vec{R}_{11}$. Indeed, the square lattice remains invariant upon the replacement $x \leftrightarrow y$.

The symmetry of the virtual electron-hole pair in Fig.3 is determined by the symmetry of the $|A_{1g}\rangle$ and $|B_{1g}\rangle$ two-hole states, since the virtual electron can only be in the state $|^1A\rangle$ of a completely occupied shell in the sector N_+ (Fig.2). The coefficients $\xi_{\vec{k}}$, $\chi_{\vec{k}}$ renormalize only the contributions with the holes in the $|B_{1g}\rangle$ states, in the hopping Hamiltonian \hat{H}_1

$$t_{\sigma}^{0,h}(\vec{R}_{ij}) \Big|_{h=|B_{1g}\rangle} = t^{p_x(p_y), d_{x^2}}(\vec{R}_{ij}) \xi(\vec{R}_{ij}) \times \dots + t^{p_x, p_y}(\vec{R}_{ij}) \chi(\vec{R}_{ij}) \times \dots \doteq \begin{cases} 0 & , \vec{R}_{ij} = \vec{R}_{11} \\ \emptyset & , \vec{R}_{ij} = \vec{R}_{10} \end{cases} \quad (6)$$

and

$$t_{\sigma}^{0,h}(\vec{R}_{ij}) \Big|_{h=|A_{1g}\rangle} = t^{p_x(p_y), d_{x^2}}(\vec{R}_{ij}) \lambda(\vec{R}_{ij}) \times \dots + t^{p_x, p_y}(\vec{R}_{ij}) \xi(\vec{R}_{ij}) \times \dots \neq 0 \quad (7)$$

at any \vec{R}_{ij} . Therefore, it is better to group the partial contributions to the total superexchange interaction \hat{H}_S not by their singlet or triplet spin nature, but by the orbital symmetry of the virtual electron-hole pair, which can be in different orbital states with the A_{1g} and B_{1g} point symmetry (see Fig.3). Thus, instead of Eq.(2) we

obtain

$$J_{tot}(\vec{R}_{ij}) = \Delta J_{AFM}^{A_{1g}}(\vec{R}_{ij}) + \Delta J_{FM}^{B_{1g}}(\vec{R}_{ij}), \quad (8)$$

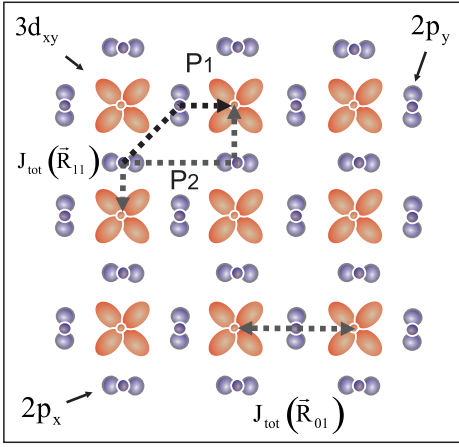


FIG. 4. Paths P_0 , P_1 and P_2 of the superexchange interactions $J_{tot}(\vec{R}_{01})$ and $J_{tot}(\vec{R}_{11})$ for the nearest and next-nearest neighbors. Here, the oxygen $2p$ orbitals π -overlap with the t_{2g} magnetic ions, and form 90° (P_1) and σ (P_2) - overlapping between themselves. The interactions $J_{tot}^{(P_1)}(\vec{R}_{11})$ and $J_{tot}^{(P_2)}(\vec{R}_{11})$ are comparable in magnitude for magnetic materials with the partially occupied t_{2g} shell.

where

$$\Delta J_{AFM}^{A_{1g}}(\vec{R}_{ij}) = \sum_{n=1}^{N_S(^1A_{1g})} |t^{0,ns}(R_{ij})|^2 / \Delta_{nS} - \sum_{m=1}^{N_T(^3A_{1g})} |t^{0,mT}(R_{ij})|^2 / \Delta_{mT}, \quad (9)$$

$$\Delta J_{FM}^{B_{1g}}(\vec{R}_{ij}) = \sum_{n=1}^{N_S(^1B_{1g})} |t^{0,ns}(\vec{R}_{ij})|^2 / \Delta_{nS} - \sum_{m=1}^{N_T(^3B_{1g})} |t^{0,mT}(\vec{R}_{ij})|^2 / \Delta_{mT},$$

The contributions $\Delta J_{AFM}^{A_{1g}}(\vec{R}_{ij})$ and $\Delta J_{FM}^{B_{1g}}(\vec{R}_{ij})$ have AFM and FM nature, respectively, due to the levels of the two-hole spin triplets $|^3A_{1g}\rangle$ and singlets $|^1B_{1g}\rangle$ lying higher in energy than the levels of the spin singlets, respectively. In fact, from Eq.(9), one finds

$$\begin{aligned} J_{tot}(\vec{R}_{01}) &= \Delta J_{AFM}^{A_{1g}}(\vec{R}_{01}) + \Delta J_{FM}^{B_{1g}}(\vec{R}_{01}) \approx (10.4 - 0.5) \times 10^{-2} eV = 9.9 \times 10^{-2} eV \\ J_{tot}(\vec{R}_{11}) &= \Delta J_{AFM}^{A_{1g}}(\vec{R}_{11}) + 0 \approx 0.2 \times 10^{-2} eV, \end{aligned} \quad (10)$$

where $\Delta J_{AFM}^{A_{1g}}(\vec{R}_{01}) \approx (15.6 - 5.2) \times 10^{-2} = 10.4 \times 10^{-2} eV$, $\Delta J_{FM}^{B_{1g}}(\vec{R}_{01}) \approx (0.4 - 0.9) \times 10^{-2} eV = -0.5 eV$

and $\Delta J_{FM}^{B_{1g}}(\vec{R}_{11}) = 0$, in the square CuO_2 layer, due to the impossibility of diagonal mobility of the virtual holes in the two-hole state $|B_{1g}\rangle$. Consequently, there is only an AFM contribution to the diagonal superexchange $J_{tot}(\vec{R}_{11})$ in Fig.3, due to the invariance of the square lattice upon the replacement $x \leftrightarrow y$ with the magnetic ion Cu^{2+} .

IV. CONCLUSIONS

To summarize, we have examined the sign and magnitude of the superexchange interaction in a CuO_2 layer between next-nearest neighbors Cu^{2+} ions. With the LDA+GTB parameters³⁶ used earlier to calculate the energy structure and ARPES spectra of HTSC cuprates we have obtained $J_{tot}(\vec{R}_{11}) \approx 9.9 \times 10^{-2} eV$. The diagonal $J_{tot}(\vec{R}_{11})$ superexchange interaction in the simple square lattice of the CuO_2 layer always has the AFM nature due to the symmetry prohibition on the FM contribution $\Delta J_{FM}^{B_{1g}}(\vec{R}_{11}) = 0$. However, there is no prohibition $\Delta J_{FM}^{B_{1g}}(\vec{R}_{01}) \approx -0.5 eV$ and $\Delta J_{FM}^{A_{1g}}(\vec{R}_{01}) \approx 10.4 \times 10^{-2} eV$ for the interacting nearest neighbors, and the AFM exchange constant $J_{tot}(\vec{R}_{ij})$ strongly decreases $J_{tot}(\vec{R}_{11})/J_{tot}(\vec{R}_{01}) \approx 0.016$ with the increasing distance between the interacting Cu^{2+} ions.

In fact, we have confirmed that there are justified reasons for considering magnetic frustrations. However, one can expect the frustrations to be negligible in most cases because of the small ratio $J_{tot}(\vec{R}_{11})/J_{tot}(\vec{R}_{01})$. In the real CuO_2 layer, square symmetry breaking can lead to the non-zero FM diagonal contribution $\Delta J_{FM}^{B_{1g}}(\vec{R}) \neq 0$, supporting the smallness of this ratio. Therefore, the transfer of the results obtained for the pseudogap at the Mott transition in the triangular lattice Hubbard model with next-nearest-neighbor hopping and magnetic frustrations³⁷ to the square CuO_2 layer is just motivating.

It is worth noting that the models $t - J$, $t - t' - J$, $t - t' - t'' - J$ with extended hopping based on the single-band approach do not contain any FM contributions, and therefore, they correctly describe magnetic interactions only in a hypothetical square lattice rather than in the real CuO_2 layer with the broken square symmetry (e.g. with tilted CuO_6 octahedra in distorted doped lattice D stripes and undoped undistorted lattice U stripes³⁸ which are controlled by spatially heterogeneous lattice microstrain^{39,40}. The internal chemical pressure in doped perovskites gives nanoscale phase separation⁴¹ and superlattices⁴². In fact, strain uncovers the interplay between two- and three-dimensional charge densities⁴³ and between the lattice superstructures and the electronic structure of cuprate perovskites⁴⁴). In gen-

eral, the type of magnetic ions remains clearly important in relation to the prohibition. This can be seen in Fig.4, where for magnetic ions with a partially occupied t_{2g} shell, the overlapping $2p$ orbitals of oxygen ions along path P_2 is quite significant and should be taken into account in calculating the diagonal superexchange constant. Further, it would be of interest to consider the effect of a certain type of broken square $x \leftrightarrow y$ symmetry with unequal lattice parameters between the orthorhombic a and b axes on the experimentally observed "Y shift"

with a surprisingly large tilt angle (the so called diagonal stripes)^{10,38–42}.

ACKNOWLEDGMENTS

We acknowledge the support of the Russian Science Foundation through grant RSF No.24-12-00044, and would like to thank Mikhailenko N.V. for assistance in preparing the manuscript for publication.

-
- ¹ J. F. Annett, R. M. Martin, A. K. McMahan, and S. Satpathy, *Phys. Rev. B* **40**, 2620 (1989).
 - ² Y. J. Kim, A. Aharony, R. J. Birgeneau, F. C. Chou, O. Entin-Wohlman, R. W. Erwin, M. Greven, A. B. Harris, M. A. Kastner, I. Y. Korenblit, Y. S. Lee, and G. Shirane, *Phys. Rev. Lett.* **83**(4), 852 (1999).
 - ³ R. Coldea, S. M. Hayden, G. Aeppli, T. G. Perring, C. D. Frost, T. E. Mason, S. W. Cheong, and Z. Fisk, *Phys. Rev. Lett.* **86**(23), 5377 (2001).
 - ⁴ V. A. Gavrichkov, S. I. Polukeev, and S. G. Ovchinnikov, *Phys. Rev. B* **95**, 144424 (2017).
 - ⁵ V. A. Gavrichkov, Z. V. Pchelkina, I. A. Nekrasov, and S. G. Ovchinnikov, *International Journal of Modern Physics B* **30**, 1650180 (2016).
 - ⁶ H. C. Jiang and T. P. Devereaux, *Science* **365**, 1424 (2019).
 - ⁷ S. R. White and D. J. Scalapino, *Phys. Rev. B* **60**, R753 (1999).
 - ⁸ C. M. Chung, M. Qin, S. Zhang, U. Schollwöck, and S. R. White, *Phys. Rev. B* **102**, 041106 (2020).
 - ⁹ M. Qin, *Phys. Rev. X* **10**, 031016 (2020).
 - ¹⁰ W. He, J. Wen, H.-C. Jiang, G. Xu, W. Tian, T. Taniguchi, Y. Ikeda, M. Fujita, and Y. S. Lee, *Commun Phys* **7**, 257 (2024).
 - ¹¹ S. Jiang, D. J. Scalapino, and S. R. White, *Phys. Rev. B* **106**, 174507 (2022).
 - ¹² M. Hartstein, Y. Hsu, K. A. Modic, J. Porras, T. Loew, M. LeTacon, H. Zuo, J. Wang, Z. Zhu, M. K. Chan, R. D. McDonald, G. G. Lonzarich, B. Keimer, S. E. Sebastian, and N. Harrison, *Nature Physics* **16**, 841–847 (2020).
 - ¹³ A. Kanigel, M. R. Norman, M. Randeria, U. Chatterjee, S. Souma, A. Kaminski, H. M. Fretwell, S. Rozenkranz, M. Shi, T. Sato, T. Takahashi, Z. Z. Li, H. Raffy, K. Kadowaki, D. Hinks, L. Ozyuzer, and C. J. C, *Nature Physics* **2**, 447 (2006).
 - ¹⁴ H. Al-Rashid and D. K. Singh, *SciPost Phys.* **16**, 107 (2024).
 - ¹⁵ K. S. Chen, Z. Y. Meng, T. Pruschke, J. Moreno, and M. Jarrell, *Phys. Rev. B* **86**, 165136 (2012).
 - ¹⁶ M. Kohno, *Phys. Rev. B* **90**, 035111 (2014).
 - ¹⁷ E. Gull, O. Parcollet, P. Werner, and A. J. Millis, *Phys. Rev. B* **80**, 245102 (2009).
 - ¹⁸ S. Wakimoto, *Phys. Rev. B* **60**, R769 (1999).
 - ¹⁹ F. M., *Phys. Rev. B* **65**, 064505 (2002).
 - ²⁰ S. R. Dunsiger, *Phys. Rev. B* **78**, 092507 (2008).
 - ²¹ V. A. Gavrichkov, S. I. Polukeev, and S. G. Ovchinnikov, *Phys. Rev. B* **101**, 094409 (2020).
 - ²² R. V. Mikhaylovskiy, T. J. Huisman, V. A. Gavrichkov, S. I. Polukeev, S. G. Ovchinnikov, D. Afanasiev, R. V. Pisarev, T. Rasing, and K. A. V, *Phys. Rev. Lett.* **125**, 157201 (2020).
 - ²³ H. Kamimura and M. Eto, *J. Phys. Soc. Jpn* **59**, 3053 (1990).
 - ²⁴ M. Eto and H. Kamimura, *Physica C Superconductivity* **185–189**, 1599–1600 (1991).
 - ²⁵ C. Janowitz, U. Seidel, R.-S. T. Unger, A. Krapf, R. Manzke, V. Gavrichkov, and S. Ovchinnikov, *JETP Letters* **80**(11), 692 (2004).
 - ²⁶ P. W. Anderson, *Phys. Rev.* **115**, 2 (1959).
 - ²⁷ K. A. Chao, J. Spalek, and A. M. Oles, *Journal of Physics C: Solid State Physics* **10**, L271 (1977).
 - ²⁸ J. Hubbard, *Proc. Roy. Soc.* **A276**, 238 (1963).
 - ²⁹ S. G. Ovchinnikov and V. V. Val'kov, *Hubbard operators in the theory strongly correlated electrons* (Imperial College Press, London, 2004) p. 241.
 - ³⁰ S. G. Ovchinnikov, V. A. Gavrichkov, M. M. Korshunov, and E. I. Shneyder, "Springer series in solid-state sciences," (Volume 171, Springer Berlin Heidelberg, Hamburg, 2012) Chap. LDA+GTB method for band structure calculations in the strongly correlated materials. In the "Theoretical Methods for strongly Correlated systems", pp. 143–171.
 - ³¹ L. F. Feiner, J. H. Jefferson, and R. Raimondi, *Phys. Rev. B* **53**, 8751 (1996).
 - ³² L. F. Feiner, J. H. Jefferson, and R. Raimondi, *Phys. Rev.Lett.* **76**, 4939 (1996).
 - ³³ V. A. Gavrichkov, S. G. Ovchinnikov, A. A. Borisov, and E. G. Goryachev, *Journal of Experimental and Theoretical Physics* **91**(2), 369 (2000).
 - ³⁴ V. Y. Irkhin and Y. P. Irkhin, *Phys. Status Solidi B* **183**, 9 (1994).
 - ³⁵ B. S. Shastry, *Phys. Rev. Lett.* **63**, 1288 (1989).
 - ³⁶ M. M. Korshunov, V. A. Gavrichkov, S. G. Ovchinnikov, I. A. Nekrasov, Z. V. Pchelkina, and V. I. Anisimov, *Phys. Rev. B* **72**, 165104 (2005).
 - ³⁷ P. O. Downey, O. Gingras, J. Fournier, C. D. Hebert, M. Charlebois, and A.-M. S. Tremblay, *Phys. Rev. B* **107**, 125159 (2023).
 - ³⁸ A. Bianconi, N. L. Saini, A. Lanzara, M. Missori, T. Rossetti, H. Oyanagi, H. Yamaguchi, K. Oka, and T. Ito, *Phys. Rev. Lett.* **76**, 3412 (1996).
 - ³⁹ A. Bianconi, N. L. Saini, S. Agrestini, D. Di Castro, and G. Bianconi, *International Journal of Modern Physics B* **14**, 3342 (2000).
 - ⁴⁰ R. Albertini, S. Macis, A. A. Ivanov, A. P. Menushenkov, A. Puri, V. Monteseguro, B. Joseph, W. Xu, A. Marcelli, P. Giraldo-Gallo, I. R. Fisher, A. Bianconi, and G. Campi, *Condensed Matter* **8**(3), 57. (2023).

- ⁴¹ K. I. Kugel, A. L. Rakhmanov, A. O. Sboychakov, N. Poccia, and A. Bianconi, *Phys. Rev. B* **78(16)**, 165124 (2008).
- ⁴² A. O. Sboychakov, K. I. Kugel, and A. Bianconi, *Condensed Matter* **7(3)**, 50 (2022).
- ⁴³ I. Vinograd, S. M. Souliou, A. A. Haghighirad, T. Lammann, Y. Caplan, M. Frachet, M. Merz, G. Garbarino, Y. Liu, S. Nakata, K. Ishida, H. M. L. Noad, M. Minola, B. Keimer, D. Orgad, C. W. Hicks, and M. Le Tacon, *Nat. Commun.* **15**, 3277 (2024).
- ⁴⁴ S. Hameed, Y. Liu, K. S. Rabinovich, G. Kim, P. Wochner, G. Christiani, G. Logvenov, K. Higuchi, N. B. Brookes, E. Weschke, F. Yakhou-Harris, A. V. Boris, B. Keimer, and M. Minola, arXiv: **2408.06774** (2024).